RESEARCH PAPER

Curcumin/Ag conjugated nanoparticles confer neuroprotection against hyoscine-induced acute psychosis: behavioral and biochemical evidence

Setayesh Abdolkarimi[1#], Mahsa Salehirad[1#], A. Wallace Hayes[2], Majid Motaghinejad[3*], Malak Hekmati[4]

[1] Department of Pharmaceutical Chemistry, Faculty of Pharmaceutical Chemistry, Tehran Medical Sciences, Islamic Azad University, Tehran, Iran
[2] University of South Florida College of Public Health, Tampa, FL, USA and Institute for Integrative Toxicology, Michigan State University, East Lansing, MI, USA
[3] Pediatric Respiratory Disease Research Center, National Research Institute of Tuberculosis and Lung Disease, Shahid Beheshti University of Medical Sciences, Tehran, Iran
[4] Department of Organic Chemistry, Faculty of Pharmaceutical Chemistry, Tehran Medical Sciences, Islamic Azad University, Tehran, Iran

 # Equal first authors

ABSTRACT

Obejctive(s): Psychosis is a prevalent psychiatric disorder. Chemicals that modulate the dopaminergic system have been the primary treatment, but these drugs have not always been effective, and some have deleterious side effects. During the last several years, a concerted effort has been made to advance the development of novel pharmaceuticals, utilizing approaches such as nanotechnology, natural compounds, and Eastern medicinal practices. Nanotechnology, including Ag-based nanoparticles, is an exciting option for optimizing drug performance, including reduced side effects and improved pharmacological and clinical profiles. The impact of curcumin-Ag conjugated nanoparticles (Cur/Ag NPs) was evaluated in a rodent model of psychosis.

Materials and Methods: Cur/Ag NPs were synthesized and characterized by FTIR, FE-SEM, EDX, and UV-vis spectrophotometry. The effect of Cur-Ag NPs was determined for several psychosis-related behaviors (Yawning number, rearing number, and stereotype score) and blood levels of the inflammatory factors CRP, TNF-α, and IL-1β, and cortisol in an animal model of hyoscine-induced psychosis.

Results: Cur/Ag NPs modulated the Yawning number, rearing number, and stereotypic score in hyoscine-induced acute psychosis and attenuated the blood levels of inflammatory parameters, including TNF-α, IL-1β, C-reactive protein, and cortisol. Cur/Ag NPs demonstrated greater efficacy compared to curcumin, altering these effects at lower concentrations.

Conclusion: Cur/Ag NPs and Curcumin were effective in a mouse model of psychosis, exhibiting protective effects against hyoscine-induced acute psychosis, and may be potential candidates for further clinical investigation for treating psychosis-related behavior.

Keywords: *Psychosis; Curcumin/Ag conjugated nanoparticles; Curcumin.*

How to cite this article
Abdolkarimi S, Salehirad M, Hayes A.W, Motaghinejad M, Hekmati M. Curcumin/Ag conjugated nanoparticles confer neuroprotection against hyoscine-induced acute psychosis: behavioral and biochemical evidence. Nanomed J. 2026; 13: 1-. DOI: 10.22038/NMJ.2026.86441.2178

ABBREVIATIONS

AD: Alzheimer Disease, **Ag:** Silver, **BSA:** Bovine Serum Albumin, **C.longa:** *Curcuma longa*, **CRP:** C-Reactive Protein, **Cur:** Curcumin, **Cur-Ag NPs:** Curcumin-silver nanoparticles, **ddH2O:** Double-distilled water, **EDS:** Energy Dispersive X-ray Spectroscopy, **ELISA:** Enzyme-Linked Immunosorbent Assay, **FESEM:** Field emission scanning electron microscope, **FTIR:** Fourier transform infrared, **GPx:** Glutathione Peroxidase, **GR:** Glutathione Reductase, **HAL:** Haloperidol, **HYO:** Scopolamine, **IL-1β:** Interleukin-1 beta, **KOH:** Potassium Hydroxide, **MAP:** Mapping Analysis, **NPs:** nanoparticles, **PD:** Parkinson Disease, **RNS:** Reactive Nitrogen Species, **ROS:** Reactive Oxygen Species, **SOD:** Superoxide Dismutase, **TNF-α:** Tumor Necrosis Factor-alpha, **UV-Vis:** ultraviolet-visible spectroscopy, **XRD:** X-ray diffractometer.

INTRODUCTION

Schizophrenia is a neurobehavioral and psychiatric disorder that involves a combination of genetics and brain chemistry [1, 2]. A proposed mechanism involves the excessive production of gamma-aminobutyric acid (GABA)- ergic neurons, which utilize GABA as their neurotransmitter. GABAergic neurons are found in

* *Corresponding author:* Majid Motaghinejad, Pediatric Respiratory Disease Research Center, National Research Institute of Tuberculosis and Lung Disease, Shahid Beheshti University of Medical Sciences, Tehran, Iran. Tel: +98 21 26109484, Fax: +98 21 26109680, Emails: Dr.motaghinejad6@gmail.com.

Note. This manuscript was submitted on March 01, 2025; approved on October 01, 2025.

the hippocampus, thalamus, basal ganglia, hypothalamus, and brainstem, significantly impacting dopamine secretion and dysfunction through the mesocortical-mesolimbic nucleus pathways [3, 4].

It has been suggested that increased dopamine levels or activity in the nucleus of the mesolimbic system is associated with the emergence of positive symptoms. At the same time, decreases are manifested as negative symptoms [5, 6]. Several models for the induction of psychosis, most of which are based on increasing dopamine and decreasing the cholinergic system, are available [7-10]. Scopolamine (hyoscine) can cause symptoms similar to acute psychosis in rodents [7-9, 11-13]. Other drugs, such as ketamine and apomorphine, induce chronic psychosis [12, 14-16]. Accordingly, and considering the pharmacological properties of hyoscine in inhibiting the cholinergic system and enhancing dopaminergic, and on substantial evidence of psychosis induction following its use in humans, as well as our pilot study and published literature [7-9, 17], we selected hyoscine as the psychosis-inducing agent for our study [7-9, 11-13].

The acute phase of schizophrenia involves altered inflammatory parameters that affect behavioral disorders [1, 2, 18, 19]. Chemicals that modulate the dopaminergic system have been the primary treatment, but these drugs have not always been effective, and some have deleterious side effects [5, 6, 20-22]. Therefore, during the last several years, research has focused on developing new drugs, including strategies employing nanotechnology, natural compounds, and Eastern medicines [23, 24].

Curcumin, the primary ingredient in turmeric, is a pharmacologically active, safe, accessible, and effective natural product [25, 26]. Curcumin demonstrates a variety of pharmacological effects, including free radical scavenging, anti-inflammatory activity, inhibition of cell proliferation, antimicrobial effects, pain relief, antimalarial activity, tumor suppression, induction of programmed cell death, and inhibition of new blood vessel formation [26-29].

Nanotechnology, including Ag-based nanoparticles [30-33], is an exciting option for optimizing drug performance, including reduced side effects and improved pharmacological and clinical profiles [30-33]. Curcumin nanoparticles as modulators of neurobehavioral and neurologic disorders such as anxiety, depression, PD, and AD have been investigated, but the involvement of curcumin nanoparticles in the management of schizophrenia and psychotic-like disorders has not been evaluated [34]. Effects exerted by curcumin-Ag conjugated nanoparticles on several inflammatory parameters were assessed in a rat model of acute psychosis.

MATERIALS AND METHODS

Agents and Materials

Curcumin, silver nitrate ($AgNO_3$), ethanol, and potassium hydroxide were obtained from Merck (New Jersey, USA). Reagents were of analytical grade and applied as supplied (DNA Co, Iran, Tehran).

Synthesis of curcumin-Ag conjugated nanoparticles

An eco-friendly method capitalizing on curcumin's reductive and stabilizing properties was used for synthesizing the curcumin-Ag conjugated nanoparticles [35, 36]. Curcumin (5mg) was dissolved in 50 mL of double-distilled water at neutral pH and heated to 85–90°C, resulting in an orange-colored solution. Fifty mL of a silver nitrate solution (0.1 M) was gradually added to the orange-colored solution, yielding a yellow-colored solution. This mixture was refluxed at 85–90°C for one hour and cooled to 4°C. The solution was brought to a pH of about 8 using potassium hydroxide (0.1 M), during which the color transitioned from yellow to pale yellow and ultimately to dark orange, accompanied by the emergence of brown, flaky precipitates.

The silver ions (Ag^+) interacted with curcumin to form a stable silver-curcumin complex, stabilizing the ions and initiating the reduction process (Equation 1). The aldehyde group in curcumin (R-CHO), the reducing agent, was oxidized to carboxylic acid (R-COOH). At the same time, the reduction of silver ions in the complex formed metallic silver nanoparticles (Equation 2). This mechanism also promoted nucleation and stabilized the nanoparticles in a colloidal state.

(1) $Ag^+(aq)$ + Curcumin → $[Ag(Curcuma.longa)]^+$

(2) $[Ag(C.longa)]^+$ + R–CHO → $[Ag(Curcuma.longa)]^+$ + R–COOH

Characterization studies of nanoparticles

The Cur/Ag NPs were characterized using analytical techniques to confirm their structural, compositional, and morphological properties. UV-Vis spectroscopy monitored the optical properties and validated the successful formation of nanoparticles by identifying characteristic plasmon resonance peaks. The crystallographic structure was determined using XRD, providing insights into the crystalline and lattice arrangement of the nanoparticles.

The Cur/Ag NPs' elemental composition and distribution were analyzed using EDS and MAP, which determined elemental ratios and their spatial dispersion within the nanoparticles. FESEM was utilized to investigate the nanoparticles' surface morphology, size, and shape, offering high-resolution visualizations of the nanoscale architecture.

FTIR identified functional groups and confirmed the interaction between curcumin and silver ions. This analysis also provided information about the nanoparticles' stability and potential surface modifications. These techniques allowed an understanding of the physicochemical properties and structural integrity of the Cur/Ag NPs.

Stability of curcumin-Ag conjugated nanoparticles

The stability of the curcumin-Ag conjugated nanoparticles is influenced by the chemical interaction between functional groups of Cur and silver ions, forming a robust bond that enhances the nanoparticle integrity. These nanoparticles exhibited remarkable stability due largely to curcumin's antioxidant and reducing properties, which prevented oxidation and agglomeration of silver particles. FTIR and XRD analyses confirmed the nanoparticles' strong coordination and crystalline structure, indicating resistance to degradation over time. Additionally, their stability was further validated by energy dispersive spectroscopy, which revealed a uniform elemental distribution. These morphological observations were confirmed through electron microscopy.

In-vivo study

Animals

One hundred and forty-four male and 50 female BALB/c mice (30–35g) were purchased from Experimental Animal Center of IUMS and held for two weeks before initiating experimental procedures. Animals have free access to water and animal special pellet feed (Parsfeed Co, Tehran, Iran). The animal house was controlled with standard room temperature: 22 ± 2°C; relative humidity: 5-40%; and light/dark cycles (12-hour). Both series of animal protocols were confirmed and approved by the ethics committees of research at the Pharmacy and Pharmaceutical Branches Faculty at Islamic Azad Tehran Medical Sciences University [Protocol and Ethical Code Number: IR. IAU.PS.REC.1398.348] [37]. Signs of toxicity were evaluated in the animals 24 hours after treatment and continuously during weeks one and two.

Experimental animal procedure

Pilot study evaluating the toxicity of the eco-friendly synthesized nanoparticles

Mice (8/sex/group) were administered intraperitoneally 1000, 1250, 1500, 1750, or 2000 mg/kg Cur/Ag NPs and observed for behavioral changes and signs of toxicity throughout the initial 24 hours and daily for two weeks. Brain, liver, heart, testes, and lungs were prepared for histopathological evaluation. This evaluation showed normal cellular architecture without evidence of inflammation, degeneration, or necrosis; thus, this nanoparticle [38, 39].

Effect of curcumin-Ag conjugated nanoparticles on behavioral and molecular changes in a rodent psychosis model (Fig. 1)

Male mice (8/group) were randomly divided into eight groups as follows:

- Group 1: received 0.2 mL of normal saline (control).
- Group 2: Hyoscine (HYO) (0.125 mg/kg).
- Group 3: HYO (0.125 mg/kg) and haloperidol (HAL) (5 mg/kg).
- Groups 4-6: HYO (0.125 mg/kg) and Cur/Ag NPs (20, 40 and 60 mg/kg).
- Group 7: HYO (0.125 mg/kg) and also Cur (40 mg/kg).
- Group 8: HYO (0.125 mg/kg) and Ag (40 mg/kg).

All treatments were given intraperitoneally (ip). The main experimental procedures, protocol and also associated timeline are schematically illustrated in Figure 1. Dose selection for HYO [10, 40-42], HAL [43-46], Cur [30, 47, 48], and Ag[49, 50] was based on the literature. Cur/Ag NPs doses were chosen based on previous results [51-53]. In groups 3–8, injections were administered at one-hour intervals. Psychosis-related behavior (Yawning number, rearing number, and stereotype score) was observed as early as one hour after drug administration in the experimental groups but not in control animals.

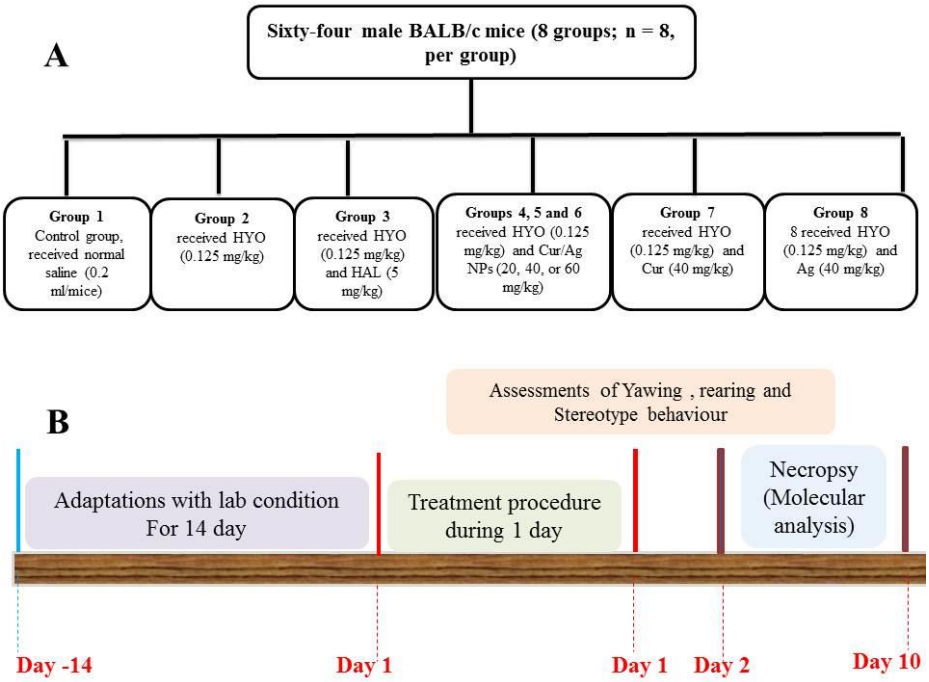

Fig. 1. (A) Schematic illustration of experimental grouping and (B) Timeline for experimental procedure and evaluation

Investigation of rearing responses induced by novelty

Central excitatory locomotor behavior was evaluated by a blinded observer using novelty-induced rearing behavior [54-56] in a transparent Plexiglas chamber (50 cm ×30 cm × 30 cm). The number of rearing was characterized by the number of standings on their hind limbs or standing with their forelimbs against the wall of the observation box or free in the air. Rearing behavior was measured over 10 minutes [54, 55]. The testing chamber was cleaned with 10% ethanol between testing runs to eliminate potential olfactory bias [54-56].

Behavioral assessment of Yawning

Yawning behavior, a standard behavior in rodents that closely mimics psychosis [56-58], is characterized by prolonged (more than 1 s) and a significant mouth opening, quickly succeeded by closure [56, 57]. This behavior was evaluated by a blinded observer observing the Yawning behavior of the mice in a transparent Plexiglas chamber (50 cm ×30 cm × 30 cm). Yawning was measured over 10 minutes, and the testing chamber was cleaned with 10% ethanol between testing runs to prevent possible olfactory interference [56-58].

Assessment of stereotypic behavior

Stereotypic behaviors are a series of standard psychosis-related behaviors that can be observed in rodents [59-61]. The signs of stereotypy sniffing and gnawing are scored as follows: absence of stereotypy was scored as 0, occasional sniffing was scored as 1, occasional sniffing with occasional gnawing was scored as 2, frequent gnawing was scored as 3, intense continuous gnawing was scored as 4, and marked gnawing activity along with staying in place was scored as 5 [59-61]. Scores are summed over 10 minutes for each animal. A blinded observer determined scores while the animals were in the transparent Plexiglas chamber (50 cm ×30 cm × 30 cm).

After the behavioral assessments, Animals were subjected to thiopental sodium-induced anesthesia (50 mg/kg) and then euthanized. Blood samples were collected directly from the heart to measure inflammatory factors such as TNF-alpha, CRP, IL-1beta, and cortisol levels. Samples were centrifuged and stored at -20 °C until analyzed.

Assessment of blood cortisol level

The cortisol concentration (µg/dL) was measured using electrochemical luminescence kits (DNA Co., Tehran, Iran) [62, 63]. Results are reported as µg/dL [62, 63].

Measurements of total protein

Total protein levels were quantified using the Bradford special assay kit (Bio-Rad, Providence, RI, USA). A standard protein curve was constructed with BSA using serially diluted BSA solutions in the range of 0.1–1.0 mg/mL. Zero, 0.5, 10, 15, 20, 25, 30, or 35 µL of serum was added to separate wells, and then the Bradford reagent was added. Using a Hiperion Microplate Reader (MPR4+, Rayto

Company, China), absorbance between 630 and 635 nm was recorded to evaluate protein content in each well [64-66].

Assessment of TNF-α, IL-1β and CRP

Commercial Enzyme-linked immunosorbent assay (ELISA) and antibody-based kits (Sino Biological Co., Eschborn, Germany) for TNF-α (SEK50349), IL-1β (50101-R001), and CRP (KIT11250A) were used to determine serum levels of CRP, TNF-α, and IL-1β. Sheep anti-mouse TNF-α, IL-1β, and CRP polyclonal antibodies (Sino Biological CO, Eschborn, Germany) were washed three times with a wash buffer (0.5M NaCl, 2.5mM $Na_{H2}PO_4$, 7.5mM Na_2HPO_4, 0.1% Tween 20), pH, 7.2. In individual wells, ovalbumin solution [100µL of 1% (w/v)] (Sigma Chemical Co., Poole, Dorset, U.K.) was added and maintained at room tmeparture with 37° C for 1.5 hours. All wells were then washed three times with the provided buffer solution. One hundred µL of standard solution or sample was added to all wells and incubated at 45 °C for 24 hours. Then, all wells were washed (3 times with the buffer), and 100 µL of sheep-based TNF-α, IL-1β, or CRP antibody was added to the appropriate wells (Antibodies diluted as 1:1000 in wash buffer containing 1% sheep serum, Sigma Chemical Co., Poole and Dorset, U.K.). All wells were incubated at room temperature for 60 minutes and washed three times with the buffer solution. Next, 100µL of Avidin-HRP (Dako Ltd, U.K.), diluted 1:5000 in wash buffer, was added to each well, followed by incubation for 20 minutes. All wells were washed (3 times) with the wash buffer, and 100µL of TMB substrate (3,3',5,5'-Tetramethylbenzidine) solution (Dako Ltd., U.K.) was added to each well and incubated (16 min) at room temperature. In the final step, 100µL of 1M H_2SO_4 was added to all wells to stop the reaction. Optical density was read at 450 nm, and results for TNF-α, IL-1β, and CRP are given in pg/mL [67-70].

Statistical analysis

All statistical evaluations and analyses were performed with special software, GraphPad PRISM v.6 (2016) (GraphPad Company, San Diego, USA). The mean ± standard deviation (SD) was calculated for all parameters and all experiments, then analyzed by a one-way ANOVA (Analysis of Variance), *F*-test. Differences and comparisons between each group were evaluated using Bonferroni's post-hoc test. The continuous variables were confirmed to follow a normal distribution by Kolmogorov-Smirnov test, and Levene's or Bartlett's test was used for analysis of variance consistency among groups. Data met ANOVA assumptions of normality (Kolmogorov-Smirnov, P>0.05) and equal variances (Levene's test, P>0.05), justifying the use of parametric tests. P<0.05 was considered significant. For each experimental parameter, the number in parentheses indicates the F (7, 56) statistic, with the subsequent P value provided.

RESULT

Cur/Ag NPs synthesis

The successful/effective synthesis of the Cur/Ag NPs was confirmed.

FT-IR spectroscopy characterization

The FT-IR spectrum of the curcumin-silver nanoparticles, illustrated in Figure 2, offers insights into the nanoparticle's chemical functionality and surface modification. Although signals associated with carbon-carbon bonds are common in organic compounds, they generate overlapping bands that are generally weak and do not provide clear diagnostic information. A broad absorption band in the 2400–3450 cm^{-1} range was observed, indicative of hydroxyl (–OH) stretching vibrations. This feature was attributed to oxidative processes introducing hydroxyl and carboxyl functional groups at the surface of the nanoparticle, which play a significant role in surface stabilization and functionalization.

A significant peak in the absorption spectrum at 1627 cm^{-1} corresponded to the stretching vibration of carbonyl (C=O) groups, while the band at 1278 cm^{-1} was assigned to C–O stretching vibrations, highlighting the presence of ester or phenolic functional groups, supporting the chemical interaction between curcumin and silver ions in forming and stabilizing the nanoparticle. The peaks at 1510 cm^{-1} and 1514 cm^{-1} were associated with the aromatic C=C stretching vibrations intrinsic to the curcumin structure. The peaks confirmed that curcumin retained its aromatic structure, which is essential for its biochemical activity.

The absorption bands at 3014 cm^{-1} and 3049 cm^{-1} represented sp^2-hybridized alkenyl (C–H) stretching vibrations, while the band at 2972 cm^{-1} indicated the presence of sp^3-hybridized aliphatic (C–H) bonds. These characteristic functional groups and vibrational modes provided an extensive insight into the molecular interactions and surface chemistry of the curcumin-silver nanoparticles. The FTIR analysis indicated a shift to lower stretching frequency values, suggesting effective coordination between curcumin's functional groups and silver ions. This shift signified strong interaction and stabilization during the nanoparticle synthesis process. These results support the successful synthesis of curcumin-silver nanoparticles.

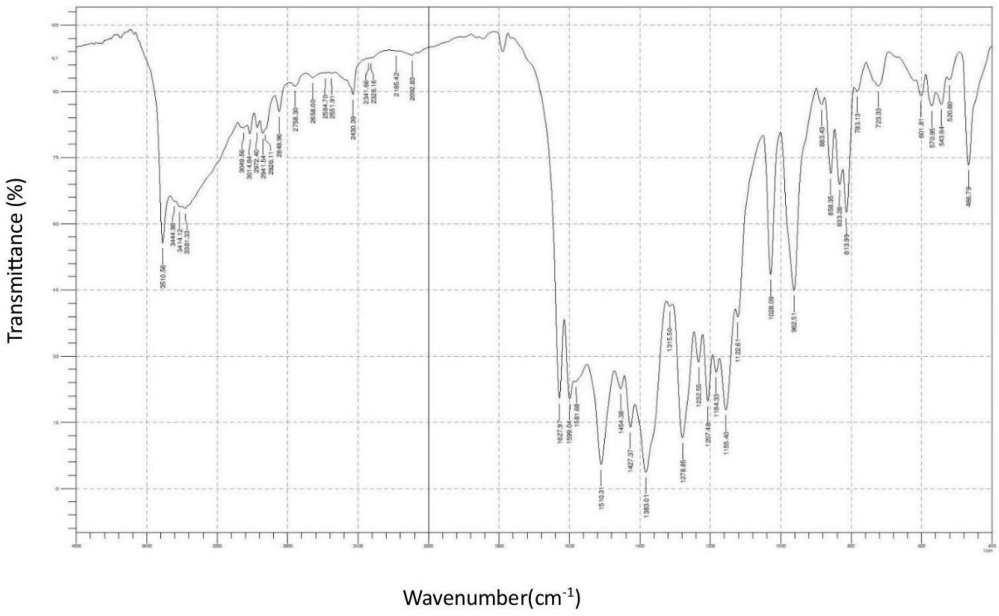

Fig. 2. FT-IR spectrum of Cur/Ag NPs

Characterization by UV–Vis spectrophotometry

The UV-Vis analysis identified a strong absorption peak at 428 nm (Figure 3), confirming the successful formation of silver nanoparticles. This peak affirmed the nanoscale size and interaction with curcumin. It also highlights the coordination between silver and curcumin's functional groups, demonstrating effective stabilization and synthesis of nanoparticles.

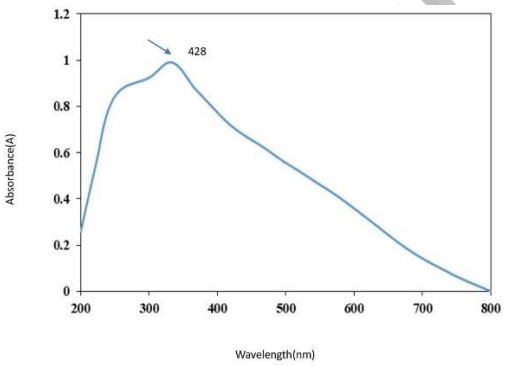

Fig. 3. UV-Vis analysis of Cur/Ag NPs

Morphological insights from FESEM and EDX studies

The FESEM (Figure 4) spectrum provided further evidence of successful nanoparticle formation. The results confirmed that curcumin effectively acted as a reducing agent, converting silver ions into silver nanoparticles. Additionally, the morphology of the nanoparticles and the identification of their constituent profile are illustrated in the following figures, offering additional validation of the structural characteristics of the curcumin-silver nanoparticles. The constituent elements of the curcumin–silver nanoparticles produced were characterized through EDS (Figure 5). EDS results validated the detection of silver (Ag), chlorine (Cl), carbon (C), nitrogen (N) and oxygen (O) as constituents of the nanoparticles. Figure 6 illustrates the elemental mapping, showcasing the presence of C, N, O, Cl, and Ag in the curcumin-silver nanoparticles. High-resolution FESEM images combined with EDS analysis further confirmed the successful incorporation of silver, revealing its even distribution throughout the curcumin matrix. This consistency highlighted the contribution of curcumin as an efficient reducing and stabilizing factor during the synthesis process. Figure 7 offers a spatial visualization of the elements, showing the successful incorporation of silver nanoparticles within the curcumin-silver framework and verifying the presence of silver while demonstrating its uniform distribution alongside carbon, nitrogen, oxygen, and chlorine.

XRD analysis

The diffraction pattern revealed the crystalline lattice structure of the silver metal nanoparticle. As shown in Figure 8, the diffraction peak at 23.8° was attributed to the presence of hexagonal graphite. The diffraction pattern exhibited strong signals at 38.1°, 44.3°, 64.4°, 77.4°, and 81.5°, consistent with silver's crystallographic planes, confirming the crystalline state of silver and the proper synthesis of curcumin–silver nanoparticle. The matching diffraction peaks with standard silver patterns further demonstrated the reliability of the synthesis process.

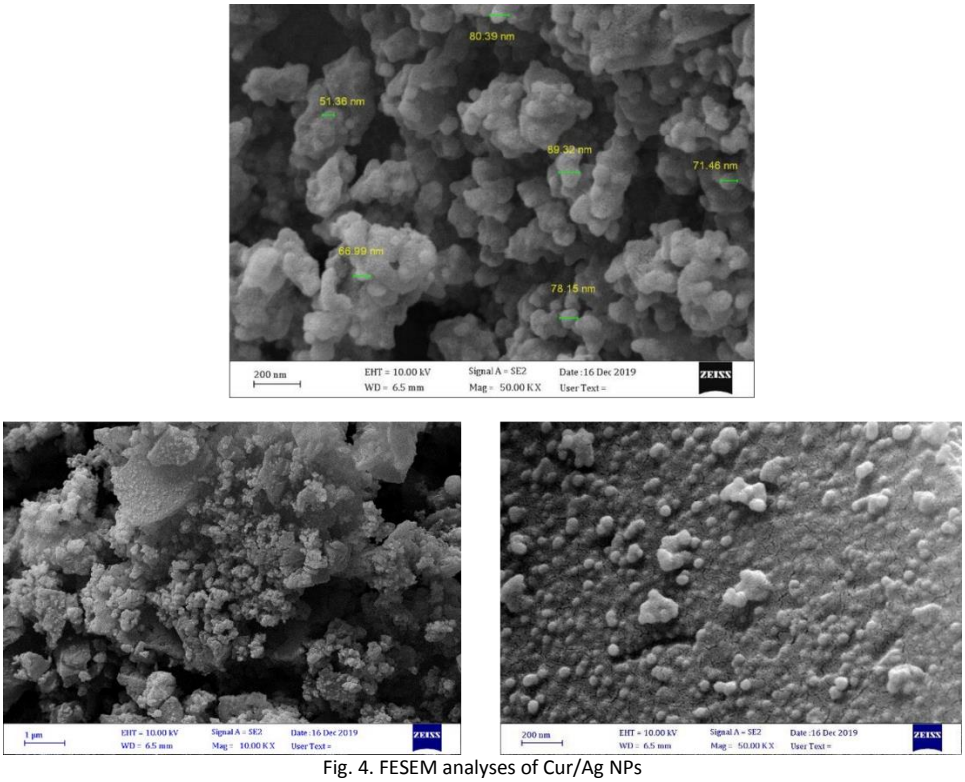

Fig. 4. FESEM analyses of Cur/Ag NPs

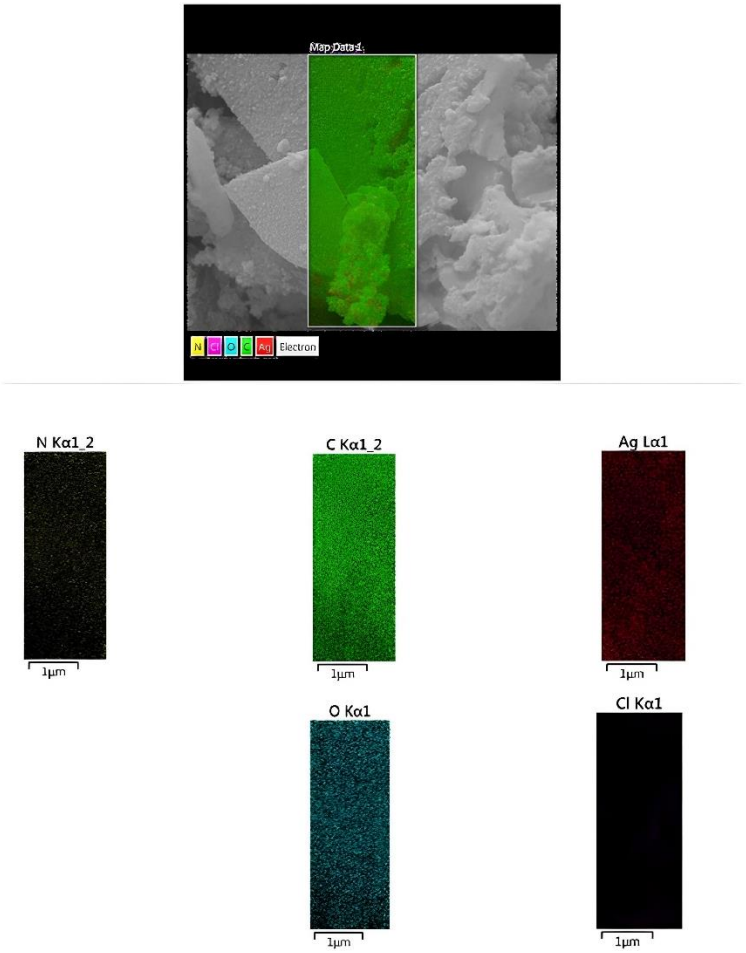

Fig. 5. EDS analyses of Cur/Ag NPs

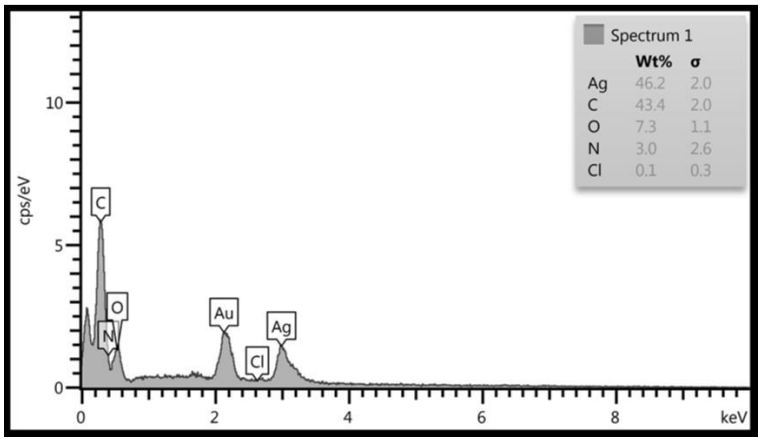

Fig. 6. Elemental mapping of Cur/Ag NPs

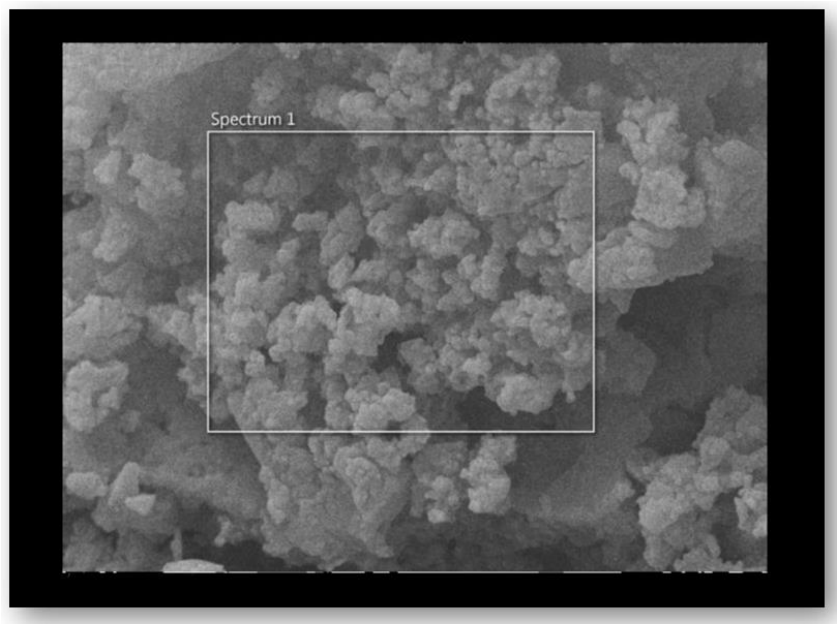

Fig. 7. FESEM combined with EDS of Cur/Ag NPs

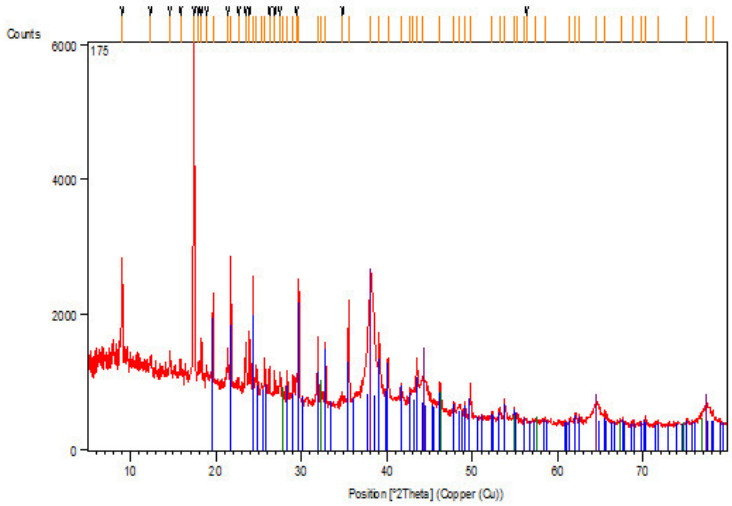

Fig. 8. XRD analyses of Cur/Ag NPs

Cur/Ag NPs effects against psychosis related behavior

Cur/Ag NPs effects on HYO-prompted CHANGES in rearing behavior

HYO (0.125 mg/kg) increased rearing number (6.600; P<0.05). HAL (5 mg/kg) reduced the rearing number in the HYO (0.125 mg/kg) treated mice (6.600; P<0.05) (Figure 9). Cur/Ag NPs with doses of 40 or 60 mg/kg reduced the rearing number in HYO-treated mice (6.600; P<0.05). Cur (40 mg/kg) and Ag (40 mg/kg) did not alter the rearing number in HYO-treated mice (Figure 9).

Cur/Ag NPs effects on HYO-prompted changes in Yawning behavior

HYO (0.125 mg/kg) increased the Yawning behavior (5.323; P<0.05) (Figure 10). HAL (5 mg/kg) reduced the Yawning behavior in HYO-treated mice (5.323; P<0.05) (Figure 10). Cur/Ag NPs with doses of 40 and 60 mg/kg also reduced Yawning behavior in the HYO-treated mice (5.323; P<0.05). Cur as 40 mg/kg and Ag, with a dose of 40 mg/kg did not change the Yawning behavior in HYO-treated mice (Figure 10).

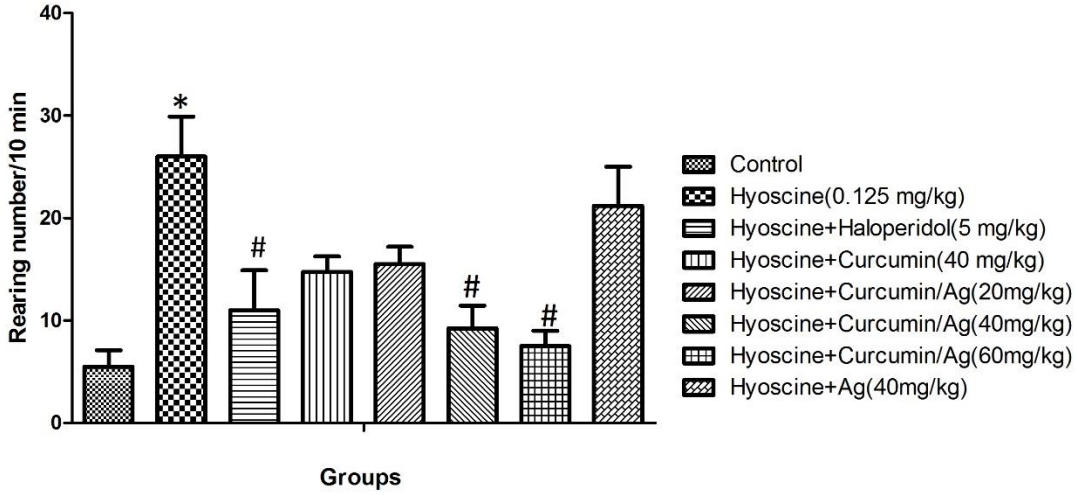

Fig. 9. Effects of Cur/Ag NPs on HYO-induced Alteration in Rearing Number.
Data are Mean ± SD (n=8). * P< 0.001 vs. control. # P< 0.001 vs. HYO (5 mg/kg).
HYO: Hyoscine, Cur: Curcumin, Cur/Ag N.P.s: Curcumin-silver nanoparticles, HAL: Haloperidol.

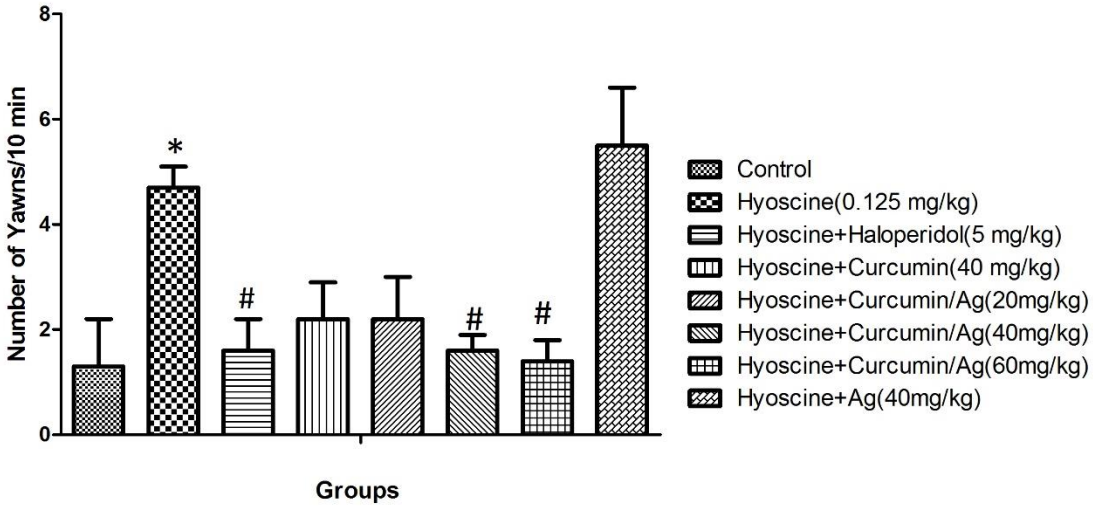

Fig. 10. Effects of Cur/Ag NPs on HYO-induced Alteration in Yawning Number.
Data are Mean ± SD (n=8). * P< 0.001 vs. control. # P< 0.001 vs. HYO (5 mg/kg).
HYO: Hyoscine, Cur: Curcumin, Cur/Ag N.P.s: Curcumin-silver nanoparticles, HAL: Haloperidol.

Cur/Ag NPs effects on HYO- HYO-prompted changes in stereotype behavior

HYO (0.125 mg/kg) increased stereotype behavior scores (4.553; P<0.05) (Figure 11). HAL (5 mg/kg) reduced the stereotype behavior scores in HYO (0.125 mg/kg) treated mice (4.553; P<0.05) (Figure 11). Cur as 40 mg/kg and Cur/Ag NPs with doses of 40 and 60 mg/kg reduced stereotype behavior scores in HYO (0.125 mg/kg) treated mice (4.553; P<0.05) (Figure 11). Ag (40 m/kg) did not change these scores in HYO (0.125 mg/kg) treated mice (Figure 11).

Cur/Ag NPs effects against psychosis related inflammatory biomarkers

Cur/Ag NPs effect on HYO-induced changes in blood cortisol level

HYO (0.125 mg/kg) increased blood cortisol levels (4.393; P<0.05) (Figure 12). HAL (5 mg/kg) reduced these levels in HYO (0.125 mg/kg) treated mice (4.393; P<0.05) (Figure 12). Cur as 40 mg/kg and Cur/Ag NPs with doses of 40 and 60 mg/kg reduced blood cortisol levels in HYO (0.125 mg/kg) treated mice (4.393; P<0.05) (Figure 12). Ag (40 m/kg) did not affect the blood cortisol levels in HYO (0.125 mg/kg) treated mice (Figure 12).

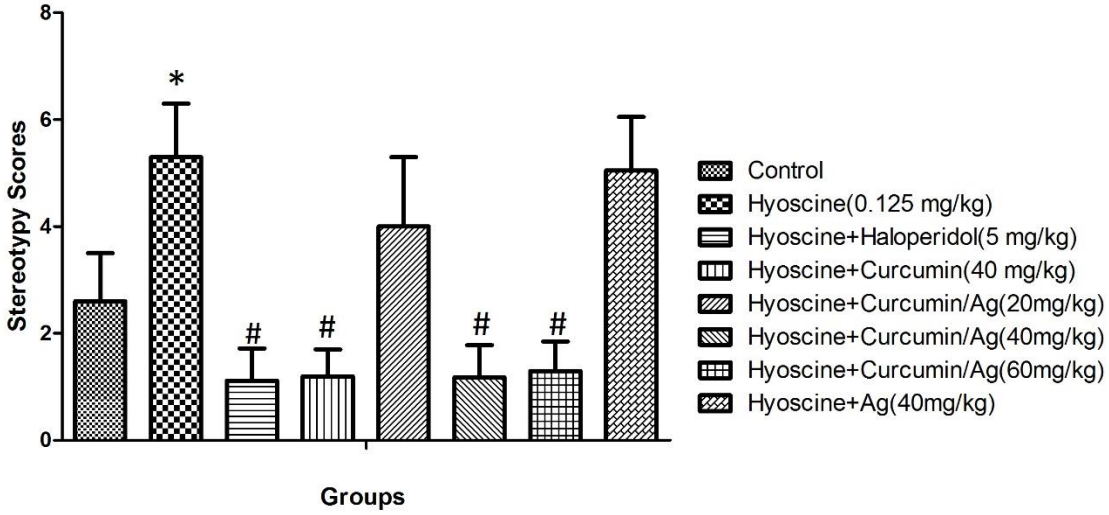

Fig. 11. Effects of Cur/Ag NPs on HYO-induced Alteration in Stereotype Score.
Data are Mean ± SD (n=8). * P< 0.001 vs. control. # P< 0.001 vs. HYO (5 mg/kg).
HYO: Hyoscine, Cur: Curcumin, Cur/Ag N.P.s: Curcumin-silver nanoparticles, HAL: Haloperidol.

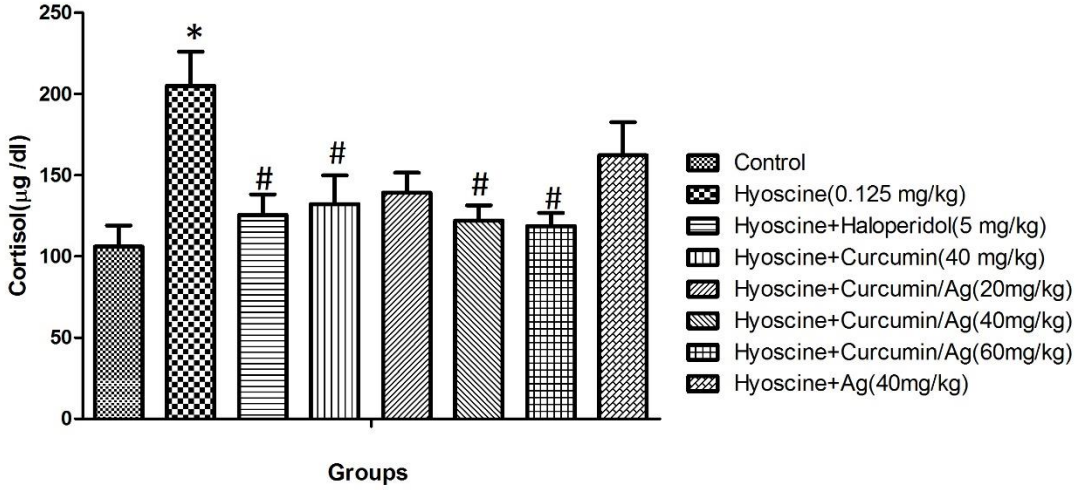

Fig. 12. Effects of Cur/Ag NPs on HYO-induced Alteration in Cortisol Level.
Data are Mean ± SD (n=8). * P< 0.001 vs. control. # P< 0.001 vs. HYO (5 mg/kg).
HYO: Hyoscine, Cur: Curcumin, Cur/Ag N.P.s: Curcumin-silver nanoparticles, HAL: Haloperidol.

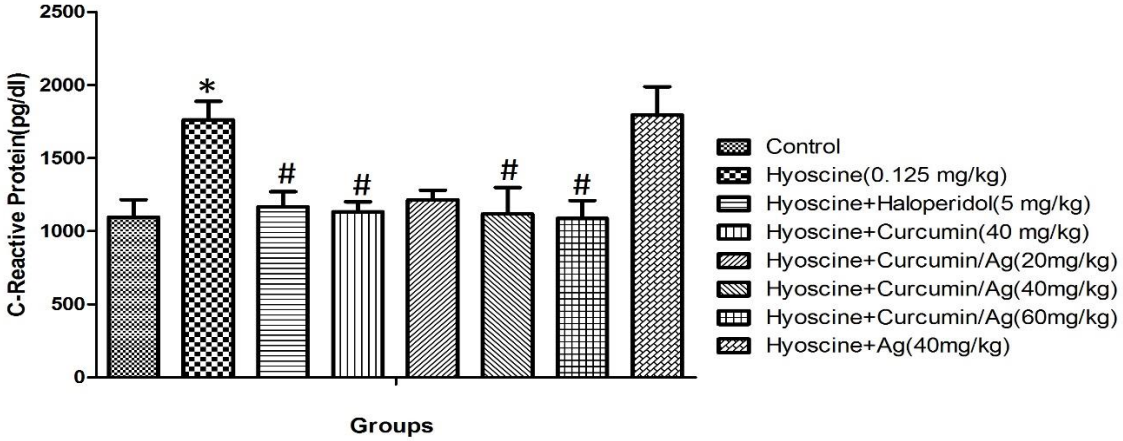

Fig. 13. Effects of Cur/Ag NPs on HYO-induced Alteration in C-reactive Protein Level.
Data are expressed as Mean ± SD (n=8). * P< 0.001 vs. control. # P< 0.001 vs. HYO (5mg/kg).
HYO: Hyoscine, Cur: Curcumin, Cur/Ag N.P.s: Curcumin-silver nanoparticles, HAL: Haloperidol.

Cur/Ag NPs effect on HYO-induced changes in blood CRP level

HYO (0.125 mg/kg) increased blood CRP levels (5.375; P<0.05) (Figure 13). HAL (5 mg/kg) reduced the blood CRP levels in HYO (0.125 mg/kg) treated mice (5.375; P<0.05) (Figure 13). Cur with doses of 40 mg/kg and Cur/Ag NPs with doses of 40 and 60 mg/kg reduced blood CRP levels in HYO (0.125 mg/kg) treated mice (5.375; P<0.05) (Figure 13). Ag (40 m/kg) did not change the blood CRP levels in HYO (0.125 mg/kg) treated mice (Figure 13).

Cur/Ag NPs effect on HYO-induced changes in blood TNF-α, IL-1β level

HYO (0.125 mg/kg) increased blood TNF-α (5.332; P<0.05) and IL-1β (6.466; P<0.05) levels (Figure 14 A and B). The analysis revealed stable levels of TNF-α in the blood (5.332) or IL-1β (6.466) in HYO (0.125 mg/kg) treated mice (Figure 14 A and B) given HAL (5 mg/kg). Cur with a dose of 40 mg/kg and Cur/Ag NPs as 40 and 60 mg/kg reduced blood TNF-α (5.332; P<0.05) and IL-1β (6.466; P<0.05) levels in HYO (0.125 mg/kg) treated mice (5.375; P<0.05) (Figure 14 A and B). Ag (40 m/kg) did not change the blood TNF-α (5.332) and IL-1β (6.466) levels in HYO (0.125 mg/kg) treated mice (Figure 14 A and B).

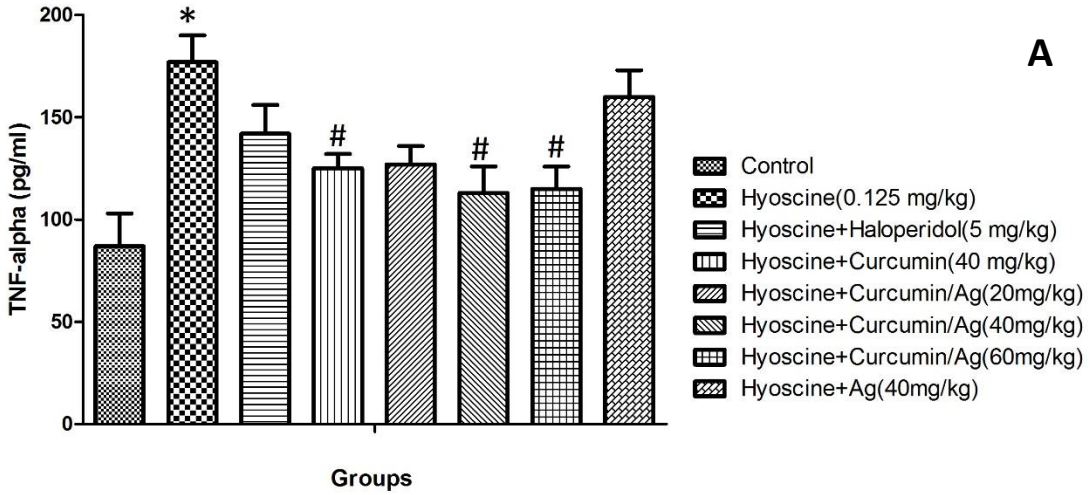

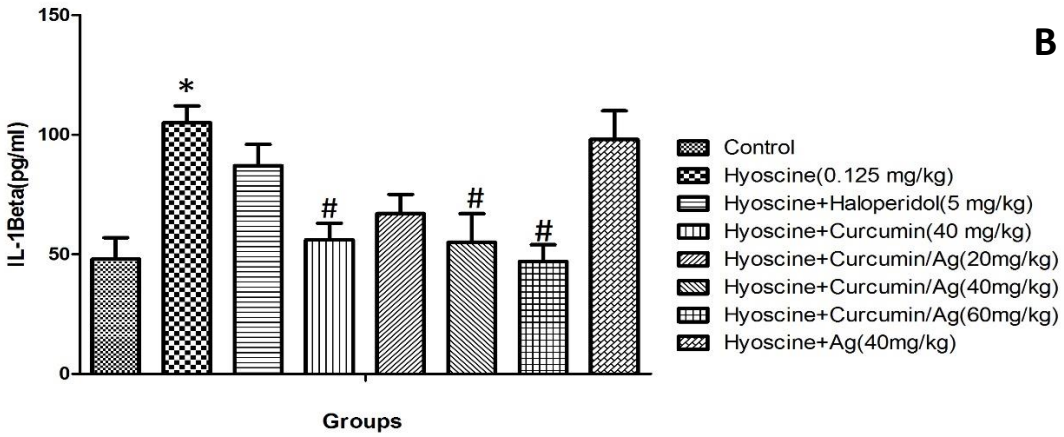

Fig.-14. Effects of Cur/Ag NPs on HYO induced alteration in TNF-α (A) and IL-1β (B) level.
Data are expressed as Mean ± SD (n=8). * P< 0.001 vs. control. # P< 0.001 vs. HYO (5mg/kg).
HYO: Hyoscine, Cur: Curcumin, Cur/Ag N.P.s: Curcumin-silver nanoparticles, HAL: Haloperidol.

DISCUSSION

As a chronic psychiatric illness, schizophrenia profoundly impacts cognitive functions, affective states, and social conduct. Managing schizophrenia requires ongoing treatment [1, 2]. Disorders of dopamine and secretion function in the nucleus of mesocortical-mesolimbic are primary mechanisms of psychosis [3, 4]. Most antipsychotic drugs, such as haloperidol (HAL), act by altering the amount and strength of dopamine and serotonin and/or their associated receptors [71, 72]. Several models, based on increasing dopamine levels and decreasing acetylcholine and glutamate, are available for the induction of psychosis in rodents [7-9, 11-13]. Hyoscine and ketamine are examples of drugs that induce acute psychosis in experimental animals. Hyoscine was used in our study to induce behavioral effects associated with acute psychosis [7-9, 11-13].

Neuroinflammation and increased systemic inflammatory status have critical roles in psychosis-related behavioral disorders [73-76]. Because of the increased inflammatory response in such disorders, new therapeutic strategies should consider targeting these molecular events [77, 78]. Thus, modulating or reducing neuroinflammation and systemic inflammation may be valuable targets for new drug development [79, 80]. Such anti-inflammatory drugs are likely to be more specific, hopefully, with fewer side effects than traditional antipsychotic drugs [79-81].

Curcumin, the active ingredient in turmeric [82, 83], has antioxidant, anti-inflammatory, and anti-cell death properties [82-85]. Curcumin as a modulator in the management of behavioral disorders, such as mood, cognitive, and motor disorders, has been suggested [85]. Curcumin, however, as an effective drug in psychotic disorders, has been less studied [25, 86]. Furthermore, its role in the management of schizophrenia and psychotic-like disorders has not been sufficiently evaluated [25, 86]. Accordingly, the role of curcumin and curcumin nanoparticles in the management of some neurobehavioral and neurologic disorders, such as anxiety, depression, PD, AD, and other similar disorders, was investigated. In our study, curcumin positively altered behavioral parameters by modulating several inflammatory pathways. Thus, it could represent a potential therapeutic option for psychosis, particularly when delivered in a nanoparticle-based formulation [25, 82, 83, 86].

Nanotechnology has significantly contributed to drug development [87, 88] by increasing drug specificity and improving pharmacodynamic efficacy, pharmacokinetic properties, and the overall pharmacologic profile [88]. Nanotechnology has also reduced adverse side effects [87, 88].

The green synthesis of our nanoparticle avoided toxic chemicals, highlighting curcumin's potential for sustainable and biocompatible production of nanoparticles. By leveraging curcumin's chemistry, this process demonstrated its applicability in nanotechnology and sustainable material science, emphasizing the importance of eco-conscious strategies in nanoparticle synthesis and showcasing curcumin as a significant contributor to green chemistry initiatives. Selected tissues from mice exposed to doses of the synthesized Cur/Ag nanoparticles as high as 2000 mg/kg daily for two weeks revealed no notable changes or tissue damage. They further displayed normal cellular architecture without evidence of inflammation, degeneration, or necrosis. These findings confirmed the non-toxic nature of Cur/Ag NPs, supporting its safety profile.

The effects of Cur/Ag NPs on several inflammatory and behavioral parameters were evaluated in the hyoscine-induced rodent model of acute psychosis. Cur/Ag NPs protected against hyoscine-induced acute psychosis in a mouse model. Cur/Ag NPs modulated the Yawning number, rearing number, and stereotypic score in the hyoscine-induced acute psychosis. Cur/Ag NPs also inhibited the blood levels of the inflammatory factors TNF-α, IL-1β, C-reactive protein, and cortisol.

HYO administration caused an increase in rearing numbers [89]. In contrast, HAL, a dopamine D2 receptor antagonist, reduced the rearing number in HYO-treated mice, which confirmed its antipsychotic role [90]. Cur/Ag NPs with doses of 40 and 60 mg/kg reduced the rearing number in HYO (0.125 mg/kg) treated mice. However, neither Cur nor Ag alone altered the rearing numbers. The nanocomposite of Cur/Ag NPs enhanced the curcumin effects and exerted an anti-psychosis role, supporting previous studies [30, 31].

Yawning behavior was increased by YOH but inhibited by HAL. The effects of YOH and HAL on Yawning behavior were consistent with previous results and confirmed the psychotic role of YOH [89] and the antipsychotic role of HAL [90]. Cur/Ag NPs with doses of 40 and 60 mg/kg reduced the Yawning behavior in HYO-treated mice. Cur as 40 mg/kg and Ag (40 mg/kg) did not change the Yawning behavior.

HYO increased the stereotype behavior scores, while HAL reduced the stereotype behavior scores in HYO-treated mice. Cur and Cur/Ag NPs reduced stereotype behavior scores in HYO-treated mice. However, our curcumin-metal nanocomposite particles enhanced the antipsychotic effects of this herbal compound (curcumin). As shown in Figures 9, 10, and 11, 40 mg/kg of curcumin and 40 mg/kg of Cur/Ag NPs positively affected rearing numbers, Yawning behavior, and stereotype behavior scores. The Cur/Ag NPs altered these parameters, however, to a greater degree than curcumin alone.

HYO increased blood cortisol and CRP levels and enhanced the blood level of TNF-α and IL-1β, and HAL reduced these inflammatory parameters. In contrast, curcumin alone and Cur/Ag NPs (40 and 60 mg/kg) decreased TNF-α, IL-1β, and attenuated CRP and blood cortisol levels in HYO-treated mice. Ag (40 m/kg) did not change cortisol, TNF-α, IL-1β, or CRP blood levels. The Cur/Ag NPs exerted their protective effects against these inflammatory parameters at lower doses (Figures 12, 13, and 14). Although some of these changes were not statistically significant, these changes, nonetheless, support the potential beneficial effects of nanoparticles [87, 88].

Earlier research has suggested that inflammatory processes are strongly involved in the development of psychosis [73-76] and that inflammation can predispose degenerative damage and subsequent behavioral disorders such as psychosis [73-76, 91]. Cytokines may be valid biomarkers of psychosis in patients with this disease [91, 92]. The development of new anti-inflammatory drugs should be designed with mechanisms that inhibit inflammatory pathways in mind [79]. Both curcumin and Cur/Ag NPs may have a place in the management of psychosis by reducing oxidative stress and free radical activity, while increasing antioxidants such as superoxide dismutase, glutathion peroxidase, and glutathione reductase, and enhancing glutathione, and reducing the levels of reactive nitrogen species and reactive oxygen species [93-96].

Curcumin nanoparticle compounds with greater potency and potentially fewer side effects can play an effective anti-inflammatory role [30, 31]. In addition to the role of oxidative stress and inflammation, cell death-related pathways such as apoptosis and autophagy play a critical role in the mechanism and pathophysiology of psychosis [96-99]. Some of the effects of curcumin and Cur/Ag NPs may be explained by their potential anti-cell death properties [95-99]. Although we did not evaluate oxidative stress and cell death-related pathways, future studies should consider these pathways. In addition, since curcumin modulates neurotransmitters such as acetylcholine, dopamine, serotonin and glutamate [96-99], both curcumin and Cur-Ag NPs may have a potential role in managing acute psychosis [100-105].

CONCLUSION

Although we did not evaluate cell death-related pathways in the present study, both curcumin and curcumin-silver nanoparticles (Cur/Ag NPs) showed antioxidant properties potentially beneficial for psychosis management, possibly through modulation of neurotransmitter systems like dopamine and serotonin (98-101). Cur/Ag NPs demonstrated efficacy at lower doses than curcumin alone in reducing psychosis-like behaviors and inflammation in the hyoscine-induced rodent model of acute psychosis, with no observed toxicity at tested doses, suggesting their promise as safe therapeutic candidates (102-107). In addition to the role of oxidative stress and inflammation, cell death-related pathways such as apoptosis and autophagy play an essential role in the pathophysiology of acute psychosis [96-99].

Additional research, works and studies are required to clarify mechanisms, chronic safety, and clinical effectiveness (95-101).

ACKNOWLEDGMENT

We are grateful for the support of the Islamic Azad University, Tehran Medical Branch. The nanocomposite synthesis was conducted in the laboratories of Dr. Malak Hekmati, and the data were part of Mrs. Setayesh Abdolkarimi's master's thesis.

FUNDING

No other financial support.

CONFLICT OF INTEREST

None to declare.

REFERENCES

1. Bishop JR, Zhang L, Lizano P. Inflammation subtypes and translating inflammation-related genetic findings in schizophrenia and related psychoses: a perspective on pathways for treatment stratification and novel therapies. Harv Rev Psychiatry. 2022;30(1):59-70.
2. Williams JA, Burgess S, Suckling J, Lalousis PA, Batool F, Griffiths SL, et al. Inflammation and brain structure in schizophrenia and other neuropsychiatric disorders: a Mendelian randomization study. JAMA Psychiatry. 2022;79(5):498-507.
3. Arciniegas DB. Psychosis. Continuum (Minneap Minn). 2015;21(3):715-736.
4. Bebbington P. Unravelling psychosis: psychosocial epidemiology, mechanism, and meaning. Shanghai Arch Psychiatry. 2015;27(2):70.
5. De Oliveira IR, Juruena M. Treatment of psychosis: 30 years of progress. J Clin Pharm Ther. 2006;31(6):523-534.
6. Demjaha A, Lappin J, Stahl D, Patel M, MacCabe J, Howes O, et al. Antipsychotic treatment resistance in first-episode psychosis: prevalence, subtypes and predictors. Psychol Med. 2017;47(11):1981-1989.
7. Barak S, Weiner I. Towards an animal model of an antipsychotic drug-resistant cognitive impairment in schizophrenia: scopolamine induces abnormally persistent latent inhibition, which can be reversed by cognitive enhancers but not by antipsychotic drugs. Int J Neuropsychopharmacol. 2009;12(2):227-241.
8. Blokland A. Cholinergic models of memory impairment in animals and man: scopolamine vs. biperiden. Behav Pharmacol. 2022;33(4):231-237.
9. Barak S, Weiner I. Scopolamine induces disruption of latent inhibition which is prevented by antipsychotic drugs and an acetylcholinesterase inhibitor. Neuropsychopharmacology. 2007;32(5):989-999.
10. Ham S, Kim TK, Chung S, Im HI. Drug abuse and psychosis: new insights into drug-induced psychosis. Exp Neurobiol. 2017;26(1):11-20.
11. Forrest AD, Coto CA, Siegel SJ. Animal models of psychosis: current state and future directions. Curr Behav Neurosci Rep. 2014;1(2):100-116.
12. Piontkewitz Y, Arad M, Weiner I. Tracing the development of psychosis and its prevention: what can be learned from animal models. Neuropharmacology. 2012;62(3):1273-1289.
13. Winship IR, Dursun SM, Baker GB, Balista PA, Kandratavicius L, Maia-de-Oliveira JP, et al. An overview of animal models related to schizophrenia. Can J Psychiatry. 2019;64(1):5-17.
14. Jones CA, Watson D, Fone K. Animal models of schizophrenia. Br J Pharmacol. 2011;164(4):1162-1194.
15. Geyer MA, Moghaddam B. Animal models relevant to schizophrenia disorders. Neuropsychopharmacology. 2002;50:690-701.
16. Yadav M, Parle M, Jindal DK, Sharma N. Potential effect of spermidine on GABA, dopamine, acetylcholinesterase, oxidative stress and proinflammatory cytokines to diminish ketamine-induced psychotic symptoms in rats. Biomed Pharmacother. 2018;98:207-213.
17. Emorinken A, Akpasubi BO, Izirein HO, Oyerinde A. Acute-onset psychosis induced by a therapeutic dose of parenteral hyoscine butylbromide: a case report. Indian J Case Reports. 2023;9(3):65-67.
18. Mongan D, Ramesar M, Focking M, Cannon M, Cotter D. Role of inflammation in the pathogenesis of schizophrenia: a review of the evidence, proposed mechanisms and implications for treatment. Early Interv Psychiatry. 2020;14(4):385-397.
19. Bergink V, Gibney SM, Drexhage HA. Autoimmunity, inflammation, and psychosis: a search for peripheral markers. Biol Psychiatry. 2014;75(4):324-331.
20. Al-Diwani AA, Pollak TA, Irani SR, Lennox BR. Psychosis: an autoimmune disease? Immunology. 2017;152(3):388-401.
21. Mondelli V, Ciufolini S, Belvederi Murri M, Bonaccorso S, Di Forti M, Giordano A, et al. Cortisol and inflammatory biomarkers predict poor treatment response in first episode psychosis. Schizophr Bull. 2015;41(5):1162-1170.
22. Fusar-Poli P, Davies C, Solmi M, Brondino N, De Micheli A, Kotlicka-Antczak M, et al. Preventive treatments for psychosis: umbrella review (just the evidence). Front Psychiatry. 2019;10:764.
23. Hoenders HR, Bartels-Velthuis AA, Vollbehr NK, Bruggeman R, Knegtering H, de Jong JT. Natural medicines for psychotic disorders: a systematic review. J Nerv Ment Dis. 2018;206(2):81-101.
24. Otimenyin SO, Ior LD. Medicinal plants used in the management of psychosis. In: Complementary Therapies. IntechOpen; 2021.
25. Miodownik C, Lerner V, Kudkaeva N, Lerner PP, Pashinian A, Bersudsky Y, et al. Curcumin as add-on to antipsychotic treatment in patients with chronic schizophrenia: a randomized, double-blind, placebo-controlled study. Clin Neuropharmacol. 2019;42(4):117-122.
26. Kucukgoncu S, Guloksuz S, Tek C. Effects of curcumin on cognitive functioning and inflammatory state in schizophrenia: A double-blind, placebo-controlled pilot trial. J Clin Psychopharmacol. 2019;39(2):182-184.

27. Sudakaran SV, Venugopal JR, Vijayakumar GP, Abisegapriyan S, Grace AN, Ramakrishna S. Sequel of MgO nanoparticles in PLACL nanofibers for anticancer therapy in synergy with curcumin/β-cyclodextrin. Mater Sci Eng C. 2017;71:620-628.
28. Motaghinejad M, Bangash MY, Hosseini P, Karimian SM, Motaghinejad O. Attenuation of morphine withdrawal syndrome by various dosages of curcumin in comparison with clonidine in mouse: possible mechanism. Iran J Med Sci. 2015;40(2):125.
29. Ahmadinasab H, Motaghinejad M, Nosratabad BA, Bozorgniahosseini S, Rostami P, Jafarabadi GS, et al. Hepatoprotection effect of curcumin against methylphenidate-induced hepatotoxicity: histological and biochemical evidences. Int J Prev Med. 2022;13(1):65.
30. Mobinhosseini F, Salehirad M, Wallace Hayes A, Motaghinejad M, Hekmati M, Safari S, et al. Curcumin-ZnO conjugated nanoparticles confer neuroprotection against ketamine-induced neurotoxicity. J Biochem Mol Toxicol. 2024;38(1):e23611.
31. Adibipour F, Salehirad M, Hayes AW, Hekmati M, Motaghinejad M. Preventive effect of ZnO-metformin nanocomposite against carbon tetrachloride-induced hepatotoxicity. Nanomed Res J. 2024;9(2):155-163.
32. Kheiri R, Koohi MK, Sadeghi-Hashjin G, Nouri H, Khezli N, Hassan MA, et al. Comparison of the effects of iron oxide, as a new form of iron supplement, and ferrous sulfate on the blood levels of iron and total iron-binding globulin in the rabbit. Iran J Med Sci. 2017;42(1):79.
33. Rai M, Pandit R, Gaikwad S, Yadav A, Gade A. Potential applications of curcumin and curcumin nanoparticles: from traditional therapeutics to modern nanomedicine. Nanotechnol Rev. 2015;4(2):161-172.
34. Moniruzzaman M, Min T. Curcumin, curcumin nanoparticles and curcumin nanospheres: a review on their pharmacodynamics based on monogastric farm animal, poultry and fish nutrition. Pharmaceutics. 2020;12(5):447.
35. Runjun S, Kumar DM, Lakshi S, Anand R, Ratul S. Conjugation of curcumin with Ag nanoparticle for improving its bioavailability and study of the bioimaging response. Nanosyst Phys Chem Math. 2021;12(4):528-535.
36. El Khoury E, Abiad M, Kassaify ZG, Patra D. Green synthesis of curcumin-conjugated nanosilver for applications in nucleic acid sensing and antibacterial activity. Colloids Surf B Biointerfaces. 2015;127:274-280.
37. Percie du Sert N, Hurst V, Ahluwalia A, Alam S, Avey MT, Baker M, et al. The ARRIVE guidelines 2.0: updated guidelines for reporting animal research. J Cereb Blood Flow Metab. 2020;40(9):1769-1777.
38. Sadeghi R, Razzaghdoust A, Bakhshandeh M, Nasirinezhad F, Mofid B. Nanocurcumin as a radioprotective agent against radiation-induced mortality in mice. Nanomed J. 2019;6(1)
39. Jantawong C, Priprem A, Intuyod K, Pairojkul C, Pinlaor P, Waraasawapati S, et al. Curcumin-loaded nanocomplexes: acute and chronic toxicity studies in mice and hamsters. Toxicol Rep. 2021;8:1346-1357.
40. Abbas MM. The effect of hyoscine on serum serotonin and acetylcholine levels and their impacts on neurobehavior in mice. Egypt J Vet Sci. 2024;1:1-6.
41. Hosseinzadeh H, Ramezani M, Akhtar Y, Ziaei T. Effects Boswellia carterii gum resin fractions on intact memory and hyoscine-induced learning impairments in rats performing the morris water maze task. Med Plants. 2010;9(34):95-101.
42. Furuie H, Yamada K, Ichitani Y. MK-801-induced and scopolamine-induced hyperactivity in rats neonatally treated chronically with MK-801. Behavioural Pharmacology. 2013;24(8):678-683.
43. Arruda MdOV, Soares PM, Honório JER, Lima RCdS, Chaves EMC, Lobato RDFG, et al. Activities of the antipsychotic drugs haloperidol and risperidone on behavioural effects induced by ketamine in mice. Sci Pharm. 2008;76(4):673-688.
44. Tada M, Shirakawa K, Matsuoka N, Mutoh S. Combined treatment of quetiapine with haloperidol in animal models of antipsychotic effect and extrapyramidal side effects: comparison with risperidone and chlorpromazine. Psychopharmacology (Berl). 2004;176(1):94-100.
45. Motaghinejad M, Motevalian M, Shabab B. Possible involvements of glutamate and adrenergic receptors on acute toxicity of methylphenidate in isolated hippocampus and cerebral cortex of adult rats. Fundamental & Clinical Pharmacology. 2017;31(2):208-225.
46. Motaghinejad O, Motaghinejad M, Motevalian M, Rahimi-Sharbaf F, Beiranvand T. The effect of maternal forced exercise on offspring pain perception, motor activity and anxiety disorder: the role of 5-HT2 and D2 receptors and CREB gene expression. J Exerc Rehabil. 2017;13(5):514-521
47. Salehirad M, Hayes AW, Motaghinejad M, Gholami M. Protective effects of curcumin/magnesium oxide nanoparticles on ketamine-induced neurotoxicity in the mouse hippocampus. Res Pharm Sci. 2025;20(3):416-433.
48. Mach CM, Mathew L, Mosley SA, Kurzrock R, Smith JA. Determination of minimum effective dose and optimal dosing schedule for liposomal curcumin in a xenograft human pancreatic cancer model. Anticancer Res. 2009;29(6):1895-1899.
49. Tiwari DK, Jin T, Behari J. Dose-dependent in-vivo toxicity assessment of silver nanoparticle in Wistar rats. Toxicol Mech Methods. 2011;21(1):13-24.
50. Perkasa DP, Arozal W, Kusmardi K, Syaifudin M, Purwanti T, Laksmana RI, et al. Toxicity and biodistribution of alginate-stabilized AgNPs upon 14-days repeated dose oral administration in mice. Appl Pharm Sci. 2024;14(6):135-146.
51. Mohammadi E, Amini SM, Mostafavi SH, Amini SM. An overview of antimicrobial efficacy of curcumin-silver nanoparticles. Nanomed Res J. 2021;6(2):105-111.

52. Loo C-Y, Rohanizadeh R, Young PM, Traini D, Cavaliere R, Whitchurch CB, et al. Combination of silver nanoparticles and curcumin nanoparticles for enhanced anti-biofilm activities. J Agric Food Chem. 2016;64(12):2513-2522.
53. Monisha K, Shilpa SA, Anandan B, Hikku G. Ethanolic curcumin/silver nanoparticles suspension as antibacterial coating mixture for gutta-percha and cotton fabric. Eng Res Express. 2023;5(2):025054.
54. Stedenfeld KA, Clinton SM, Kerman IA, Akil H, Watson SJ, Sved AF. Novelty-seeking behavior predicts vulnerability in a rodent model of depression. Physiol Behav. 2011;103(2):210-216.
55. Ghafarimoghadam M, Mashayekh R, Gholami M, Fereydani P, Shelley-Tremblay J, Kandezi N, et al. A review of behavioral methods for the evaluation of cognitive performance in animal models: current techniques and links to human cognition. Physiol Behav. 2022;244:113652.
56. Yadav M, Kumar A. Behavioural and Non-behavioural Experimental Models of Psychosis: Current State and Future Aspects. Animal Models for Neurological Disorders. 2021:65-77.
57. Li S-M, Collins GT, Paul NM, Grundt P, Newman AH, Xu M, et al. Yawning and locomotor behavior induced by dopamine receptor agonists in mice and rats. Behav Pharmacol. 2010;21(3):171-181.
58. Daquin G, Micallef J, Blin O. Yawning. Sleep Med Rev. 2001;5(4):299-312.
59. Kostrzewa RM, Kostrzewa JP, Kostrzewa RA, Kostrzewa FP, Brus R, Nowak P. Stereotypic progressions in psychotic behavior. Neurotox Res. 2011;19:243-252.
60. Dahlen A, Zarei M, Melgoza A, Wagle M, Guo S. THC-induced behavioral stereotypy in zebrafish as a model of psychosis-like behavior. Sci Rep. 2021;11(1):15693.
61. Martin RS, Secchi RL, Sung E, Lemaire M, Bonhaus DW, Hedley LR, et al. Effects of cannabinoid receptor ligands on psychosis-relevant behavior models in the rat. Psychopharmacology (Berl). 2003;165:128-135.
62. Gong S, Miao Y-L, Jiao G-Z, Sun M-J, Li H, Lin J, et al. Dynamics and correlation of serum cortisol and corticosterone under different physiological or stressful conditions in mice. PLoS One. 2015;10(2):e0117503.
63. Sentari M, Harahap U, Sapiie TWA, Ritarwan K. Blood cortisol level and blood serotonin level in depression mice with basil leaf essential oil treatment. Open Access Maced J Med Sci. 2019;7(16):2652.
64. Bose U, Broadbent JA, Juhász A, Karnaneedi S, Johnston EB, Stockwell S, et al. Protein extraction protocols for optimal proteome measurement and arginine kinase quantitation from cricket Acheta domesticus for food safety assessment. Food Chem. 2021;348:129110.
65. Fernández-Vizarra E, Fernández-Silva P, Enríquez JA. Isolation of mitochondria from mammalian tissues and cultured cells. In: Cell Biology. Elsevier; 2006; 69-77.
66. Kruger NJ. The Bradford method for protein quantitation. In: The Protein Protocols Handbook. 2009:17-24.
67. Kirby DM, Thorburn DR, Turnbull DM, Taylor RW. Biochemical assays of respiratory chain complex activity. Methods Cell Biol. 2007;80:93-119.
68. Bénit P, Goncalves S, Dassa EP, Brière J-J, Martin G, Rustin P. Three spectrophotometric assays for the measurement of the five respiratory chain complexes in minuscule biological samples. Clin Chim Acta. 2006;374(1-2):81-86.
69. Hnasko R. ELISA. Springer; 2015
70. Crowther JR. The ELISA guidebook. Springer Science & Business Media; 2008.
71. Willner K, Vasan S, Patel P, Abdijadid S. Atypical antipsychotic agents. StatPearls [Internet]. StatPearls Publishing; 2024.
72. Meltzer HY, Gadaleta E. Contrasting typical and atypical antipsychotic drugs. Focus. 2021;19(1):3-13.
73. Misiak B, Bartoli F, Carrà G, Stańczykiewicz B, Gładka A, Frydecka D, et al. Immune-inflammatory markers and psychosis risk: A systematic review and meta-analysis. Psychoneuroendocrinology. 2021;127:105200.
74. Dunleavy C, Elsworthy RJ, Upthegrove R, Wood SJ, Aldred S. Inflammation in first-episode psychosis: the contribution of inflammatory biomarkers to the emergence of negative symptoms, a systematic review and meta-analysis. Acta Psychiatr Scand. 2022;146(1):6-20.
75. Kose M, Pariante CM, Dazzan P, Mondelli V. The role of peripheral inflammation in clinical outcome and brain imaging abnormalities in psychosis: a systematic review. Front Psychiatry. 2021;12:612471.
76. Ullah I, Awan HA, Aamir A, Diwan MN, de Filippis R, Awan S, et al. Role and perspectives of inflammation and C-reactive protein (CRP) in psychosis: an economic and widespread tool for assessing the disease. Int J Mol Sci. 2021;22(23):13032.
77. Zajkowska Z, Mondelli V. First-episode psychosis: an inflammatory state? Neuroimmunomodulation. 2014;21(2-3):102-108.
78. Fraguas D, Díaz-Caneja CM, Ayora M, Hernández-Álvarez F, Rodríguez-Quiroga A, Recio S, et al. Oxidative stress and inflammation in first-episode psychosis: a systematic review and meta-analysis. Schizophr Bull. 2019;45(4):742-751.
79. Jeppesen R, Christensen RH, Pedersen EM, Nordentoft M, Hjorthøj C, Köhler-Forsberg O, et al. Efficacy and safety of anti-inflammatory agents in treatment of psychotic disorders–A comprehensive systematic review and meta-analysis. Brain Behav Immun. 2020;90:364-380.
80. Çakici N, Van Beveren N, Judge-Hundal G, Koola M, Sommer I. An update on the efficacy of anti-inflammatory agents for patients with schizophrenia: a meta-analysis. Psychol Med. 2019;49(14):2307-2319.
81. Hong J, Bang M. Anti-inflammatory strategies for schizophrenia: a review of evidence for therapeutic applications and drug repurposing. Clin Psychopharmacol Neurosci. 2020;18(1):10.

82. Karthikeyan A, Senthil N, Min T. Nanocurcumin: A promising candidate for therapeutic applications. Front Pharmacol. 2020;11:487.
83. Hassanizadeh S, Shojaei M, Bagherniya M, Orekhov AN, Sahebkar A. Effect of nano-curcumin on various diseases: a comprehensive review of clinical trials. Biofactors. 2023;49(3):512-533.
84. Peng Y, Ao M, Dong B, Jiang Y, Yu L, Chen Z, et al. Anti-inflammatory effects of curcumin in inflammatory diseases: status, limitations and countermeasures. Drug Des Devel Ther. 2021;15:4503-4525.
85. Hussain Z, Thu HE, Amjad MW, Hussain F, Ahmed TA, Khan S. Exploring recent developments to improve antioxidant, anti-inflammatory and antimicrobial efficacy of curcumin: A review of new trends and future perspectives. Mater Sci Eng C Mater Biol Appl. 2017;77:1316-1326.
86. Rabiee R, Hosseini Hooshiar S, Ghaderi A, Jafarnejad S. Schizophrenia, curcumin and minimizing side effects of antipsychotic drugs: possible mechanisms. Neurochem Res. 2023;48(3):713-724.
87. Teleanu DM, Chircov C, Grumezescu AM, Volceanov A, Teleanu RI. Blood-brain delivery methods using nanotechnology. Pharmaceutics. 2018;10(4):269.
88. Naqvi S, Panghal A, Flora S. Nanotechnology: a promising approach for delivery of neuroprotective drugs. Front Neurosci. 2020;14:494.
89. Bulut NS, Arpacıoğlu ZB. Acute onset psychosis with complex neurobehavioural symptomatology following the intramuscular injection of hyoscine butylbromide: a case report with an overview of the literature. Eur J Hosp Pharm. 2022;29(5):294-297.
90. Dold M, Samara MT, Li C, Tardy M, Leucht S. Haloperidol versus first-generation antipsychotics for the treatment of schizophrenia and other psychotic disorders. Cochrane Database Syst Rev. 2015;1:CD009831
91. Perry BI, Upthegrove R, Thompson A, Marwaha S, Zammit S, Singh SP, et al. Dysglycaemia, inflammation and psychosis: findings from the UK ALSPAC birth cohort. Schizophr Bull. 2019;45(2):330-338.
92. Park S, Miller BJ. Meta-analysis of cytokine and C-reactive protein levels in high-risk psychosis. Schizophr Res. 2020;226:5-12.
93. Silva-Buzanello RA, Souza MF, Oliveira DA, Bona E, Leimann FV, Cardozo Filho L, et al. Preparation of curcumin-loaded nanoparticles and determination of the antioxidant potential of curcumin after encapsulation. Polimeros. 2016;26:207-214.
94. Scuto MC, Mancuso C, Tomasello B, Ontario ML, Cavallaro A, Frasca F, et al. Curcumin, hormesis and the nervous system. Nutrients. 2019;11(10):2417.
95. Jin W, Botchway BO, Liu X. Curcumin can activate the Nrf2/HO-1 signaling pathway and scavenge free radicals in spinal cord injury treatment. Neurorehabil Neural Repair. 2021;35(7):576-584.
96. Mittal A, Nagpal M, Vashistha VK, Arora R, Issar U. Recent advances in the antioxidant activity of metal-curcumin complexes: a combined computational and experimental review. Free Radic Res. 2024;58(1):11-26.
97. Yang C, Han M, Li R, Zhou L, Zhang Y, Duan L, et al. Curcumin nanoparticles inhibiting ferroptosis for the enhanced treatment of intracerebral hemorrhage. Int J Nanomedicine. 2021;16:8049-8065.
98. Prasad S, DuBourdieu D, Srivastava A, Kumar P, Lall R. Metal–curcumin complexes in therapeutics: an approach to enhance pharmacological effects of curcumin. Int J Mol Sci. 2021;22(13):7094.
99. Yan H, Wang L, Mu Y. Biosynthesis of Ag/Cu nanocomposite mediated by Curcuma longa: evaluation of its antibacterial properties against oral pathogens. Open Chem. 2024;22(1):20240059.
100. Khadrawy YA, Hosny EN, Magdy M, Mohammed HS. Antidepressant effects of curcumin-coated iron oxide nanoparticles in a rat model of depression. Eur J Pharmacol. 2021;908:174384.
101. Yavarpour-Bali H, Ghasemi-Kasman M, Pirzadeh M. Curcumin-loaded nanoparticles: A novel therapeutic strategy in treatment of central nervous system disorders. Int J Nanomedicine. 2019:4449-4460.
102. He X, Zhu Y, Wang M, Jing G, Zhu R, Wang S. Antidepressant effects of curcumin and HU-211 coencapsulated solid lipid nanoparticles against corticosterone-induced cellular and animal models of major depression. Int J Nanomedicine. 2016:4975-4990.
103. Sandhir R, Yadav A, Mehrotra A, Sunkaria A, Singh A, Sharma S. Curcumin nanoparticles attenuate neurochemical and neurobehavioral deficits in experimental model of Huntington's disease. Neuromolecular Med. 2014;16(1):106-118.
104. Fahmy HM, Aboalasaad FA, Mohamed AS, Elhusseiny FA, Khadrawy YA, Elmekawy A. Evaluation of the therapeutic effect of curcumin-conjugated zinc oxide nanoparticles on reserpine-induced depression in Wistar rats. Biol Trace Elem Res. 2024;202(6):2630-2644.
105. Naserzadeh P, Hafez AA, Abdorahim M, Abdollahifar MA, Shabani R, Peirovi H, et al. Curcumin loading potentiates the neuroprotective efficacy of Fe3O4 magnetic nanoparticles in cerebellum cells of schizophrenic rats. Biomed Pharmacother. 2018;108:1244-1252.